J. metamorphic Geol., 2006, **24,** 603–613 doi:10.1111/j.1525-1314.2006.00657.x

Partial high-pressure aragonitization of micritic limestones in an accretionary complex, Tavşanlı Zone, NW Turkey

G. TOPUZ,[1] A. I. OKAY,[1] R. ALTHERR,[2] H.-P. MEYER[2] AND L. NASDALA[3,*]
[1]*Eurasian Institute of Earth Sciences, Istanbul Technical University, TR-34469 Ayazağa, Istanbul, Turkey (topuzg@itu.edu.tr)*
[2]*Institute of Mineralogy, University of Heidelberg, Im Neuenheimer Feld 236, D-69120 Heidelberg, Germany*
[3]*Institute of Geosciences, University of Mainz, Becherweg 21, D-55099 Mainz, Germany*

ABSTRACT Pelagic micritic limestones within an upper Cretaceous accretionary complex in the Tavşanlı Zone, NW Turkey, preserve textures indicating incomplete prograde transformation of micritic calcite to aragonite, representing the only known example of this type. Aragonitization starts at the central parts of the micritic limestone beds and advances towards the lower and upper parts of the layers at the expense of micrite. Micrite is very fine grained (< 0.003 mm) and contains radiolaria, foraminifera and thin shell fragments. Aragonite forms large crystals, up to 3 cm across, with straight grain boundaries and c-axis mostly subparallel to the carbonate beds. Relict micritic portions are devoid of any aragonite grain. Stylolites characterized by the accumulation of clay minerals, Fe-Mn-hydroxides and quartz are concentrated in the upper and lower parts of the beds. Stylolite formation precedes aragonitization. Conditions of aragonitization are estimated as 200 ± 50 °C and 0.45–0.65 GPa, based on metamorphic mineral assemblages observed in associated basalts. Several features such as (i) constant composition of micritic calcite (98–99 mol.% $CaCO_3$) throughout individual beds, (ii) enormous grain size difference between micritic calcite and aragonite (up to 1200 times), and (iii) absence of any aragonite grains within the relict micritic portions suggest that kinetic rather than thermodynamic factors controlled selective aragonite formation in the central portions of carbonate layers.

Key words: aragonite; calcite-aragonite transition; high-pressure metamorphism; incipient blueschist-facies; Tavşanlı Zone; Turkey.

INTRODUCTION

Magmatism, seismicity and fluid flow in subduction zones are ultimately linked to mineral reactions occurring in the subducting slab. Although phase equilibria in subducting slabs are relatively well understood (e.g. Kerrick & Connolly, 2001; Poli & Schmidt, 2002; Hacker *et al*., 2003), the reaction kinetics are much less so. Especially during low-temperature metamorphism, reaction kinetics can be more important than thermodynamics in controlling pressures and temperatures of a reaction. In the absence of a catalyst such as fluid or deformation, low-pressure minerals can persist metastably well above their stability limits because of sluggish nucleation, slow diffusion, and slow growth rates (e.g. Rubie, 1998).

The polymorphic transformation of calcite to aragonite involving a volume decrease of 7%, is one of the key reactions occurring in subduction zones during HP-LT metamorphism of carbonate-bearing rocks. Most of current knowledge on the mechanism and kinetics of this transformation has been derived from experimental studies (e.g. Newton *et al*., 1969; Hacker *et al*., 1992, 2005; Hacker & Kirby, 1993; Lin & Huang, 2004). Although aragonite has been described from a number of HP-LT metamorphic terranes (e.g. Brown *et al*., 1962; Coleman & Lee, 1962; McKee, 1962; Brothers, 1970; Okay, 1982; Sakakibara, 1986; Gillet & Goffé, 1988; Franz & Okrusch, 1992; Theye & Seidel, 1993), evidence of prograde calcite to aragonite transformation, in other words 'primary sedimentary calcite together with newly formed metamorphic aragonite has not been described from the rocks. The present study reports on a so far unique occurrence of partially aragonitized micritic limestones from an accretionary complex in the Tavşanlı zone, NW Turkey, and discusses it in terms of transformation mechanism and kinetics.

GEOLOGICAL AND TECTONIC FRAMEWORK

The Tavşanlı Zone in NW Turkey is a Cretaceous HP-LT metamorphic belt, more than 250 km long and 40 km wide (Fig. 1a,b), formed through the subduction and accretion of a Neotethyan ocean and passive continental margin (e.g. Okay, 1982, 1986; Sherlock *et al*., 1999; Droop *et al*., 2005). It consists of three major tectonic units traceable throughout the whole belt (Fig. 1b). These are from bottom to top: (i) a continental micaschist-marble sequence of mainly lawsonite-blueschist-facies, (ii) an oceanic accretionary

**Present address*: Institute of Mineralogy and Crystallography, University of Vienna, Althanstr. 14, A-1090 Wien, Austria.

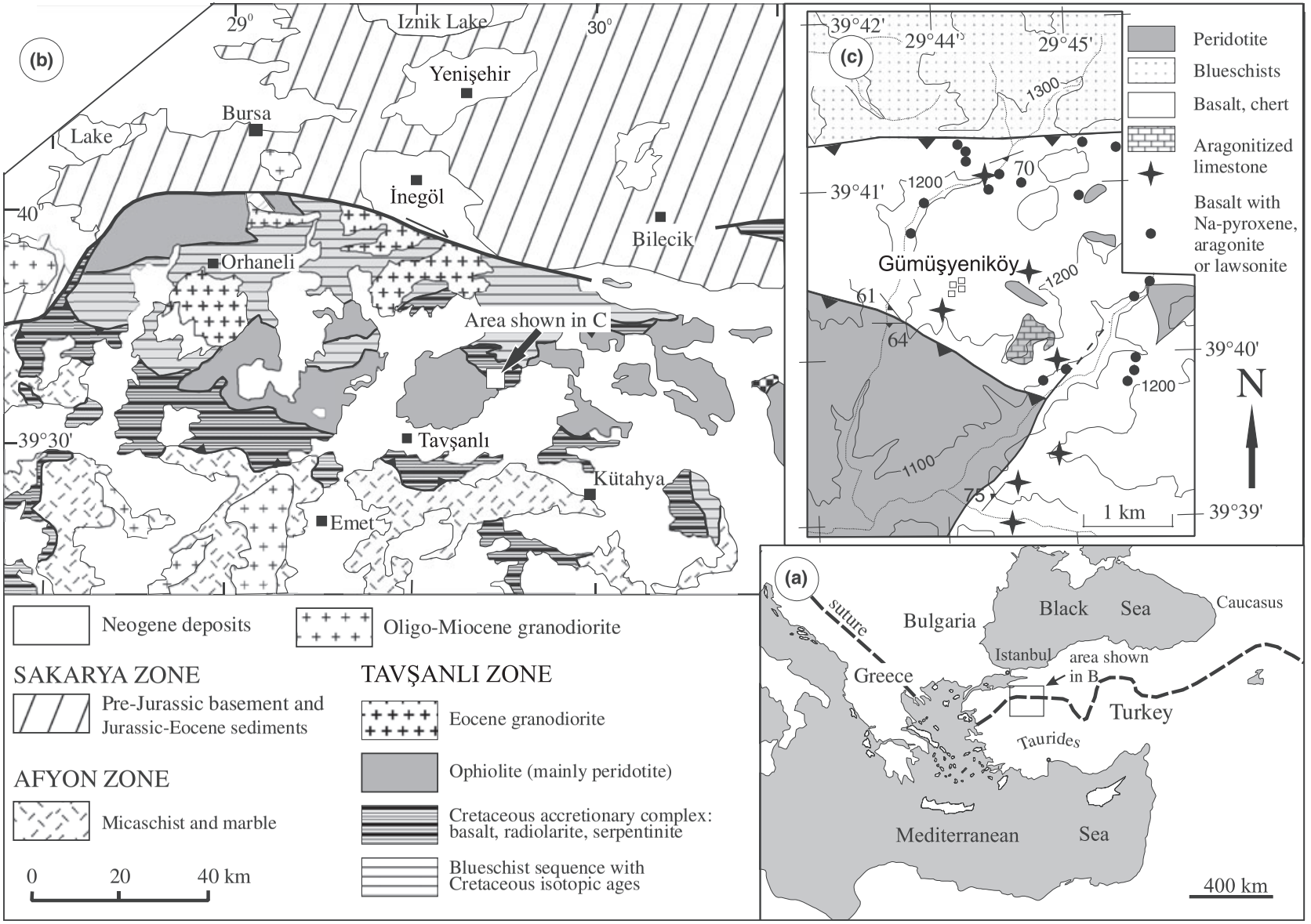

Fig. 1. (a) Location of the Tavşanlı Zone in western Turkey. Dashed line marks the Izmir-Ankara suture. (b) Geological map of the Tavşanlı Zone (modified after Okay, 2002). (c) Geological map of the Gümüşyeniköy area with sample locations.

complex with incipient blueschist-facies metamorphism, and (iii) a peridotite slab with local garnet amphibolites at its base.

The oceanic accretionary complex, often referred to as ophiolitic mélange, is characterized by tectonically juxtaposed slices, ten to hundreds of metres in thickness, consisting of basalt, red radiolarian chert, serpentinite, greywacke, shale, limestone, bedded manganese ore and rare blocks of amphibolite, microgabbro and peridotite (Okay, 1982, 1986). The accretionary complex is generally free of penetrative deformation. Locally developed penetrative fabric is confined to distinct shear zones and to tectonic contacts with the peridotite slab and the underlying blueschist-facies metaclastics-marble sequence.

Two types of aragonite-bearing carbonates are found in the accretionary complex. The first type are white, massive marble blocks in basalt, 10–30 m across, locally characterized by large rod-shaped calcite pseudomorphs after aragonite, similar to those described from Syros by Brady *et al*. (2004). The second type, the topic of this paper, are reddish limestone blocks characterized by a prominent bedding. Individual beds are 10–40 cm thick and are separated from each other by thin (< 2 cm) shaly interlayers. Locally, 10–45 cm thick chert beds occur (Fig. 2a).

We studied the reddish aragonitized limestones in several outcrops north-east of Tavşanlı in the vicinity of the village Gümüşyeniköy (Fig. 1c). In the largest outcrop, extensively quarried for local building stone, the aragonitized limestones crop out over an area of 750×500 m, have a minimum thickness of 50 m, and are underlain by basaltic pillow lavas. The interstices of the pillows are also filled by red micritic limestone (Fig. 2b). Strike and dip of the limestone bedding vary at small distances because of local folding. Apart from these large outcrops, there are numerous occurrences of smaller aragonite-bearing limestone blocks (Fig. 1c). The accretionary complex around the aragonitized limestones consists mainly of basaltic pyroclastics. The basalts contain igneous augite accompanied by chlorite, albite and titanite. Metamorphic minerals, such as lawsonite, pumpellyite, sodic pyroxene and aragonite occur in veins and amygdales of the basalts (Okay, 1982).

ANALYTICAL TECHNIQUES

The microtextural features of the carbonates were studied by transmitted-light optical microscopy and scanning electron microscopy. Cathodoluminescence imaging (hot cathode attached to an optical microscope) was used to determine different generations of calcite and aragonite. The carbonates were analysed by electron microprobe using an accelerating voltage of 15 kV, beam current of 10 nA and a beam diameter of ~ 15 μm, in order to avoid evaporation. Counting times were 10 s for Ca, Mg, Fe and Mn, and 40 s for Sr. Synthetic and natural standards were used for calibration. Raw data were corrected for matrix effects with the help of the PAP algorithm (Pouchou & Pichoir, 1984, 1985). Detection limits were 0.08 wt% FeO, 0.03 wt% MgO, 0.10 wt% MnO, 0.03 wt% CaO and 0.07 wt% SrO.

Micron-sized grains of mineral polymorphs with the same chemical composition, such as the three $CaCO_3$ polymorphs calcite, aragonite, and vaterite, can be identified and, thus, easily distinguished using Raman spectroscopy (e.g. Urmos *et al*., 1991; Behrens *et al*., 1995; Martinez-Ramirez *et al*., 2003; Balz *et al*., 2005). Raman spectra were acquired using a Horiba Jobin Yvon HR800 spectrometer system equipped with Olympus BX41 optical microscope and Peltier-cooled charge-coupled device detector. A grating with 1800 grooves per mm was placed in the optical pathway to disperse the scattered light for analysis. Spectra were excited with the 6328 Å emission of a He-Ne laser. The laser power (measured behind the microscope objective) was ~ 3 mW, which is well below the threshold for any spectral changes, or local sample decomposition, because of temperature increase caused by heavy light absorption. The Raman system was operated in the confocal mode. Using the Olympus 50× objective (numerical aperture 0.75), the lateral resolution of point measurements was on the order of 3 μm. The wave number accuracy was better than 0.5 cm^{-1}, and the spectral resolution was ~ 0.8 cm^{-1}. For more experimental details see Nasdala *et al*. (2005). A typical Raman spectrum obtained on one of the samples investigated is shown in Fig. 3. Aragonite and calcite are most easily identified and distinguished by their different low-frequency vibrations (Raman bands below 300 cm^{-1}). The two $CaCO_3$ polymorphs show also clear differences in the CO_3 bending region around 700 cm^{-1}, where the aragonite has a triplet of low-intensity bands whereas the higher-symmetric calcite shows only one band (see detail enlargements of spectra in Fig. 3).

In addition to cathodoluminescence imaging and micro-Raman spectroscopy, X-ray diffraction analysis was applied for general mineral assignment in bulk rock samples (CuKα, step: 0.02°, step time: 1 s). All major aragonite peaks between 20° and 55° (2 Θ) and those of calcite and quartz were identified.

PETROGRAPHY AND MINERAL COMPOSITIONS

Aragonitized portions of the carbonate rocks are easily recognized by their coarse grain size and their reddish colour as opposed to the grey or reddish brown colour of the micritic domains with calcite I (Fig. 2c,d). In most beds, aragonitization starts in the central parts and proceeds towards the upper and lower surfaces at the expense of micritic domains (Fig. 2c,d). Rarely, a 'spot-like' aragonitization was observed within the central parts of the beds (Fig. 2e,f). In all cases, the reaction front between aragonitized and micritic domains is irregular. This pattern of incomplete replace-

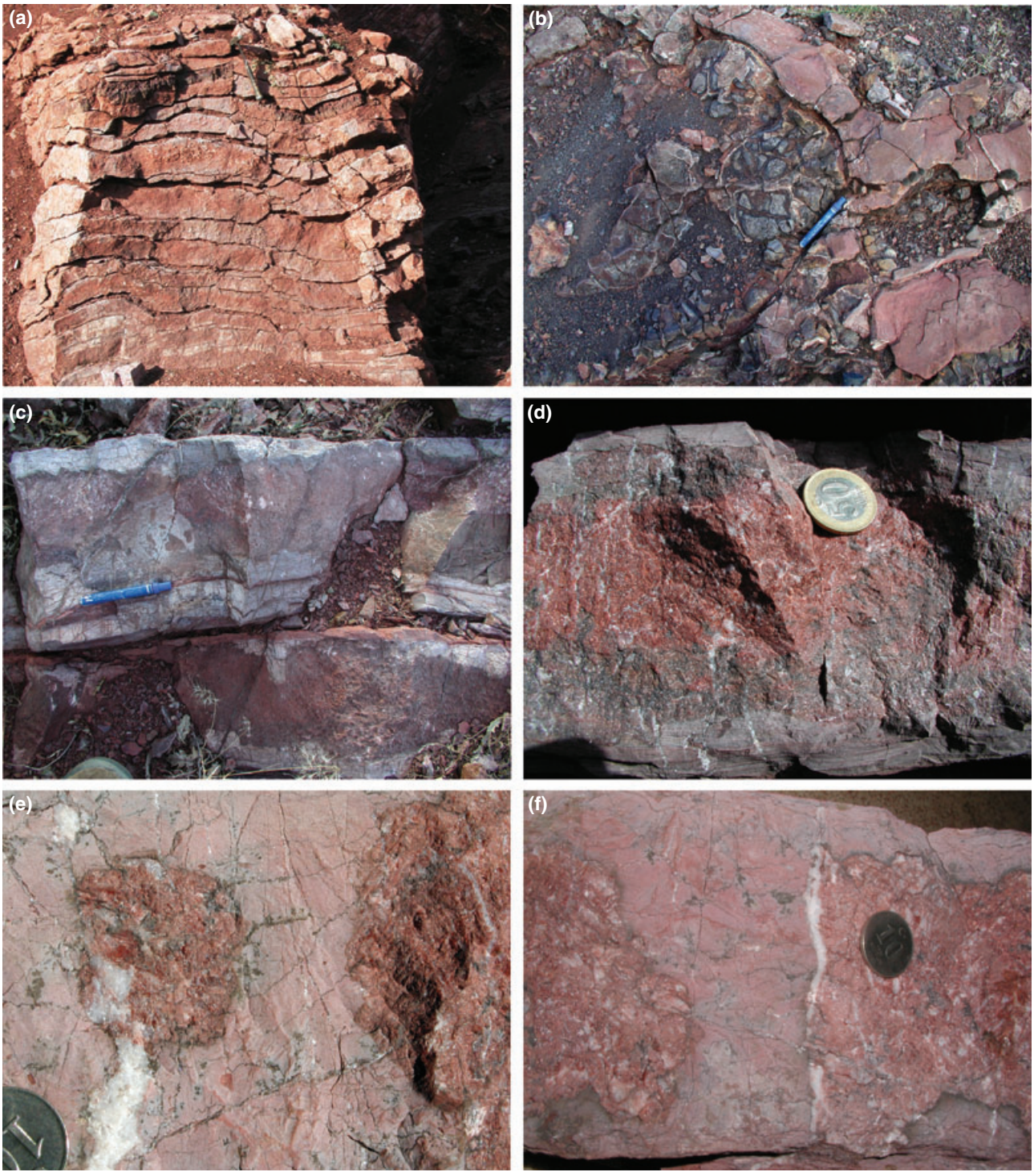

Fig. 2. (a) Appearance of aragonitized limestone in the ophiolitic mélange in the Gümüşyeniköy area. Carbonate-rich layers are separated by recessive shaly layers; in the upper part of the block, a chert layer cut by a dextral near-vertical fault is visible (near hammer). (b) Basaltic pillow (right hand side) in contact with aragonitized limestones (reddish brown). (c) Mesoscopic picture of partially aragonitized micritic limestone bed. The middle part of the layer consists of large reddish aragonite grains, while the grey fine-grained upper and lower parts are made of relict micritic limestone. (d) Hand specimen from a limestone bed. Note that the aragonitization front against the relict micritic upper and lower parts of the bed is irregular. Late-stage white calcite III veins crosscut both parts. (e) Spot-like aragonitization. Traces of former stylolites can still be recognized in the aragonitized portions. Both micritic and aragonitized rock portions are cut by veins of white calcite III. (f) Partial aragonitization of the central portion of a limestone bed. Note recessive shaly layer at the bottom.

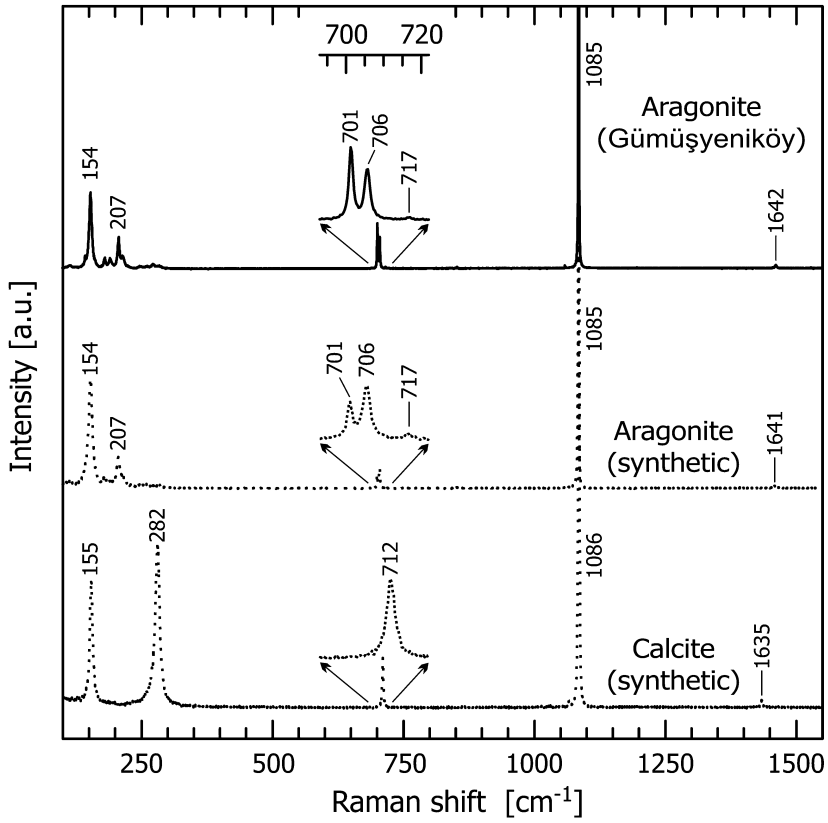

Fig. 3. Raman spectrum of aragonite ('Gümüşyeniköy'). For comparison, spectra of reference calcite and aragonite are shown.

ment is observed in over 40 individual beds in the village quarries. Complete aragonitization or lack of aragonitization is found in only a few beds.

The apparent bedding planes of the limestones coincide with grooves or thin shaly recessive layers (<2 cm thick) which are often at the centre of a zone of concentrated stylolites. Size and number of stylolites tend to decrease away from the recessive shaly layers. A close inspection under the scanning electron microscope revealed that the stylolites represent accumulations of clay minerals, Fe-Mn-hydroxides and quartz (Fig. 4a,b). Whole-rock X-ray fluorescence analyses of thin rock segments taken along a vertical profile across one complete limestone bed show that SiO_2, TiO_2, Al_2O_3, Fe_2O_3, MgO, MnO and the trace elements V, Zn, Ni and Zn increase away from the central to the upper and lower parts of the bed, consistent with an increase of the fractions of quartz, clay minerals and Fe-Mn-hydroxides (Table 1). Therefore, it is possible that the thickness of the shaly interlayers may have increased because of preferential dissolution of calcite.

Micritic portions of the carbonate beds are composed of fine-grained calcite (Cal I) with dispersed quartz (grain size ≤ 25 μm), whereby quartz makes up <10 vol.% (Fig. 5a–d). In addition, accessory apatite, very fine-grained Fe-Mn-hydroxides and some clay minerals occur. Radiolaria, unidentified foraminifera and thin shell fragments are common within the micrite (Fig. 5b), and filled with relatively coarser grains of calcite (up to 80 μm). Stylolite surfaces locally truncate radiolaria tests and shell fragments. Additionally, the micrite is crosscut by early 30–40 μm thick calcite veins, which macroscopically cannot be followed into the aragonitized sections. Under the polarizing microscope, however, some of these veins are visible as 'ghost veins', forming part of large aragonite crystals. These 'ghost veins' differ from their surrounding by the lack of impurities. A thorough examination of micritic portions by micro-Raman spectroscopy revealed general absence of aragonite. Micritic domains are slightly reddish luminescent and microveins display brighter reddish colours (Fig. 6a,b). Micritic Cal I is generally characterized by relatively high concentrations of $MgCO_3$, $MnCO_3$ and $FeCO_3$, irrespective of its position within the beds (i.e. upper and lower *v.* central parts of the beds; Table 2).

Aragonite forms large crystals (up to 3 cm in length) with straight grain boundaries and polysynthetic twinning (Figs 5d–f & 6c). The [001] direction of the aragonite grains is mainly aligned subparallel to the bedding planes. Tiny fluid inclusions (<5 μm) may be present and occur along healed cracks, testifying to their secondary nature. Large grains of aragonite may terminate at or overgrow stylolite surfaces. In the latter case, originally continuous stylolites become 'disrupted' and quartz, clay minerals and Fe-Mn-hydroxides are concentrated within short segments of relict stylolite. These features indicate that stylolite formation preceded aragonitization. Fine-grained quartz

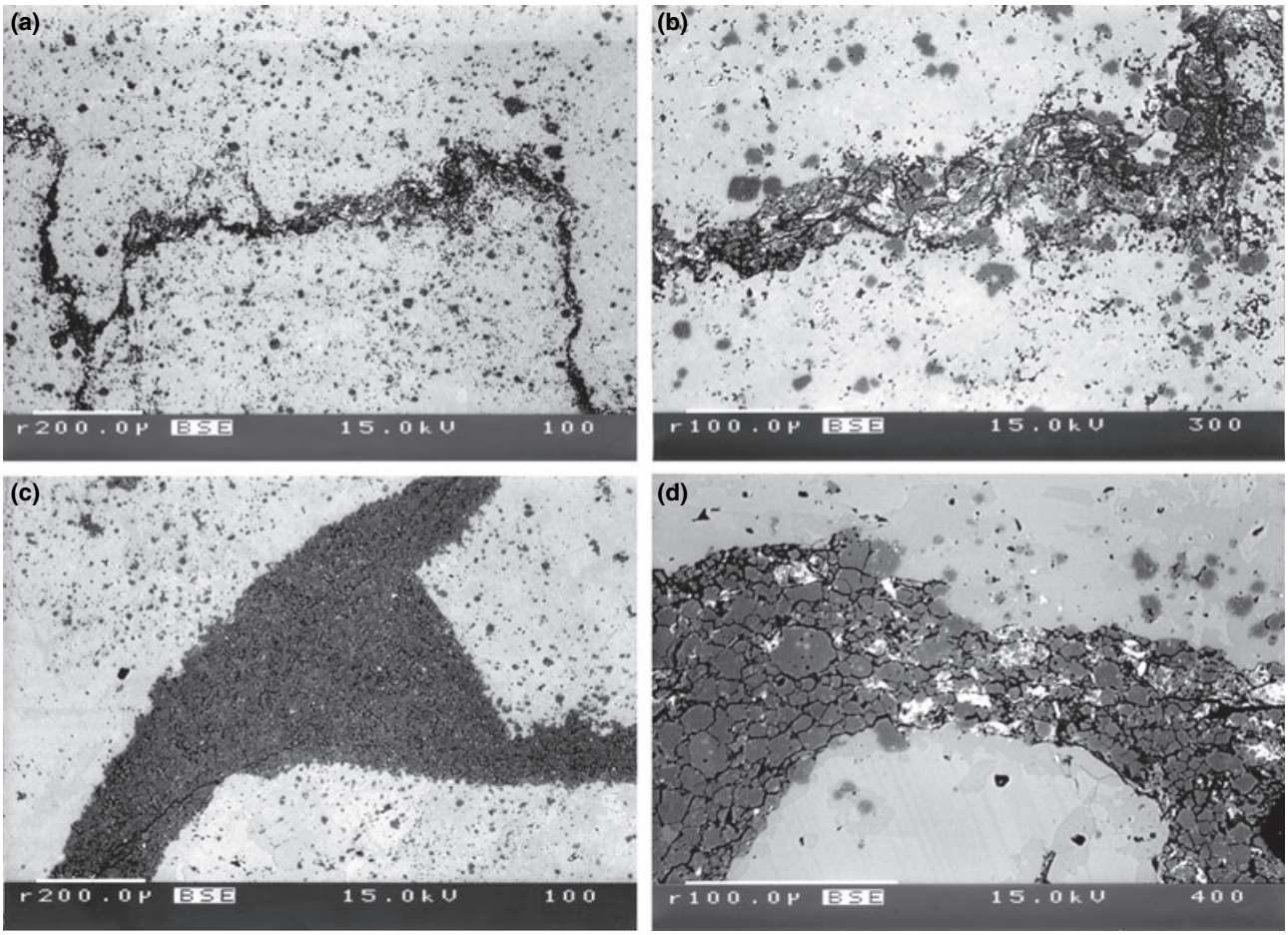

Fig. 4. (a) Back-scattered electron (BSE) image of typical stylolite in micritic portion of limestone bed. (b) Enlarged portion of panel a, with quartz (grey), Fe-Mn-hydroxides (white) and clay minerals (dark). (c) Accumulation of quartz, Fe-Mn-hydroxides and clay minerals in triple junction between large aragonite crystals. (d) Enlarged image of intergranular accumulation of quartz (grey), Fe-Mn-hydroxide (white) and clay minerals (dark) between two large aragonite crystals.

Table 1. Partial whole-rock X-ray fluorescence analyses of thin rock segments taken along a vertical profile across a limestone bed.

Sample	GT-1a	GT-1b	GT-1c	GT-1d	GT-1e
SiO_2	7.63	3.15	2.84	3.54	5.11
TiO_2	0.06	0.01	0.01	0.01	0.03
Al_2O_2	1.43	0.22	0.12	0.28	0.89
Fe_2O_2	3.83	0.47	0.47	0.66	1.94
MgO	0.93	0.27	0.17	0.33	0.78
MnO	0.77	0.39	0.03	0.44	0.68
V	40	22	8	53	30
Zn	68	16	18	18	53
Co	< 10	< 10	< 10	< 10	< 10
Ni	29	15	9	17	31
Y	40	10	11	20	25
Sr	96	315	277	126	99
Pb	13	8	9	11	9
Ba	< 10	13	< 10	< 10	< 10

Oxides in wt%, trace elements in p.p.m.w. Fe_2O_3 corresponds to total Fe. Samples GT-1a and GT-1e represent the top and bottom of the limestone layer, respectively. Both samples consist of micritic calcite, accompanied by minor quartz, smectite and Fe-Mn hydroxides. GT-1c corresponds to the middle part of the limestone bed where aragonitization is complete. Here, the amount of quartz, smectite and Fe-Mn hydroxides is lowest.

(≤25 μm) occurs either as inclusions in the aragonite or is concentrated along grain boundaries and in triple junctions, forming bands up to 150 μm across (Figs 4c,d & 5f). These accumulations of quartz are also rich in Fe-Mn-hydroxide and clay minerals. The amount of fine-grained quartz within aragonite crystals is smaller than that in the micrite. Aragonite has end-member composition with $FeCO_3$, $MgCO_3$, $MnCO_3$ and $SrCO_3$ contents below detection limits (Table 2) and is nonluminescent (Fig. 6c,d). The reddish colour of the aragonitized portions of the carbonate layers (Fig. 2) is due to intergranular Fe-Mn-hydroxides coating the aragonite crystals. Large aragonite crystals, when broken, appear white to transparent (Fig. 2f).

Aragonite is locally replaced by late fine to coarse-grained (≤1000 μm) calcite (Cal II) with end-member composition (Table 2). Cal II is locally reddish-orange luminescent (Fig. 6b). The carbonate beds, including the micritic and aragonitized portions, are steeply cut by late carbonate veins (up to 2 cm thick), consisting of calcite (Cal III) grains (100–400 μm) with straight to

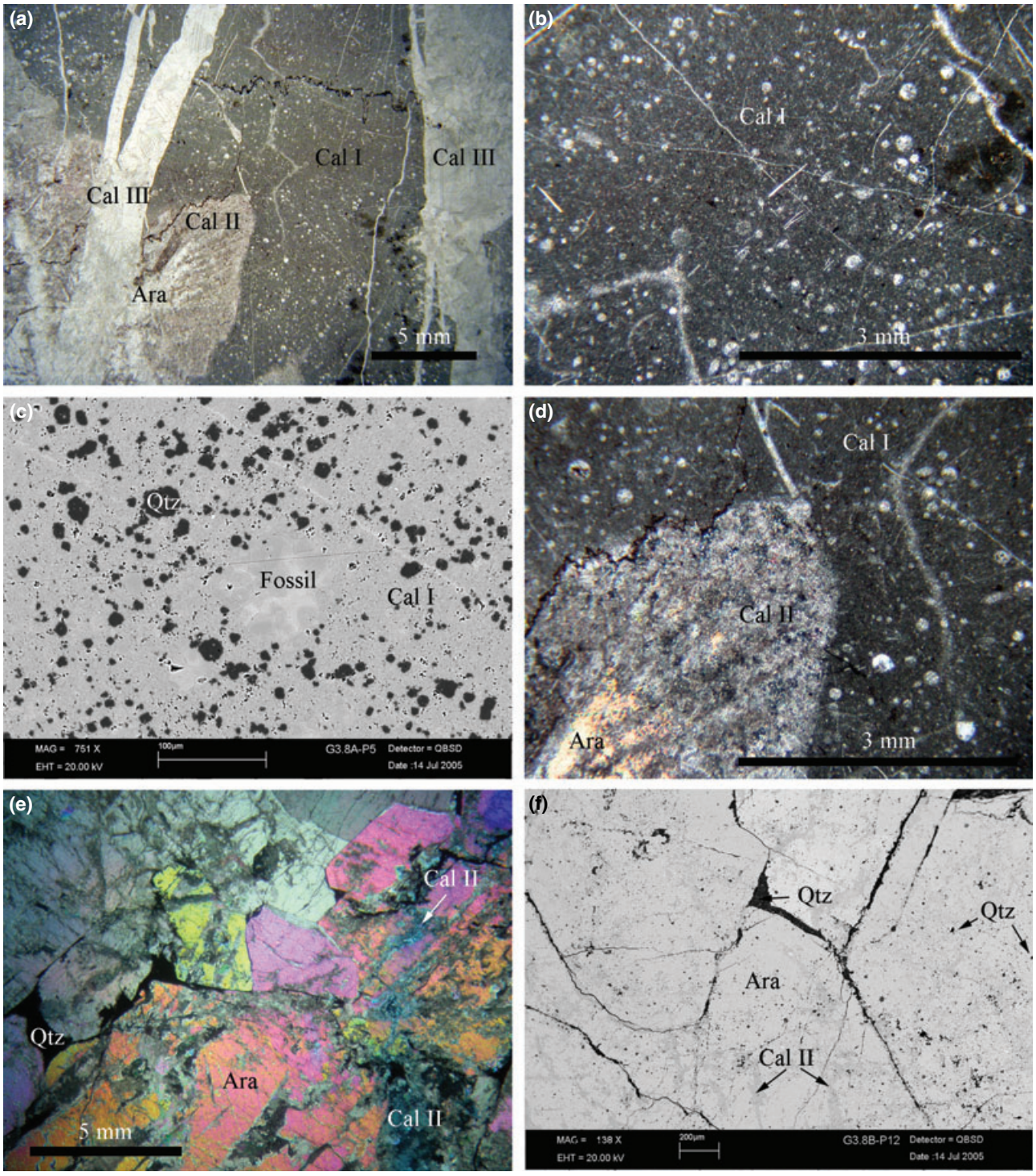

Fig. 5. (a) Micritic limestone (Cal I) with metamorphic aragonite (Ara) partly transformed to calcite (Cal II). Late-stage veins of calcite (Cal III) are younger than stylolites. (b) Enlarged microscopic picture of relict micrite with radiolaria and foraminifera, cut by early thin veins. (c) Back-scattered electron image of relict micrite with dark quartz (Qtz) bright calcite (Cal I) and fossil. (d) Detail from panel a with boundary between metamorphic aragonite (partly transformed to calcite II) and micrite (Cal I). (e) Coarse-grained aragonite grains with straight boundaries meeting in triple points and intergranular quartz (Qtz). Aragonite is partly replaced by secondary calcite (Cal II). Crossed polarizers. (f) Back-scattered electron image of coarse-grained aragonite (Ara) partly replaced by secondary calcite (Cal II). Quartz (Qtz) occurs along grain boundaries between aragonite crystals as well as inclusion in aragonite.

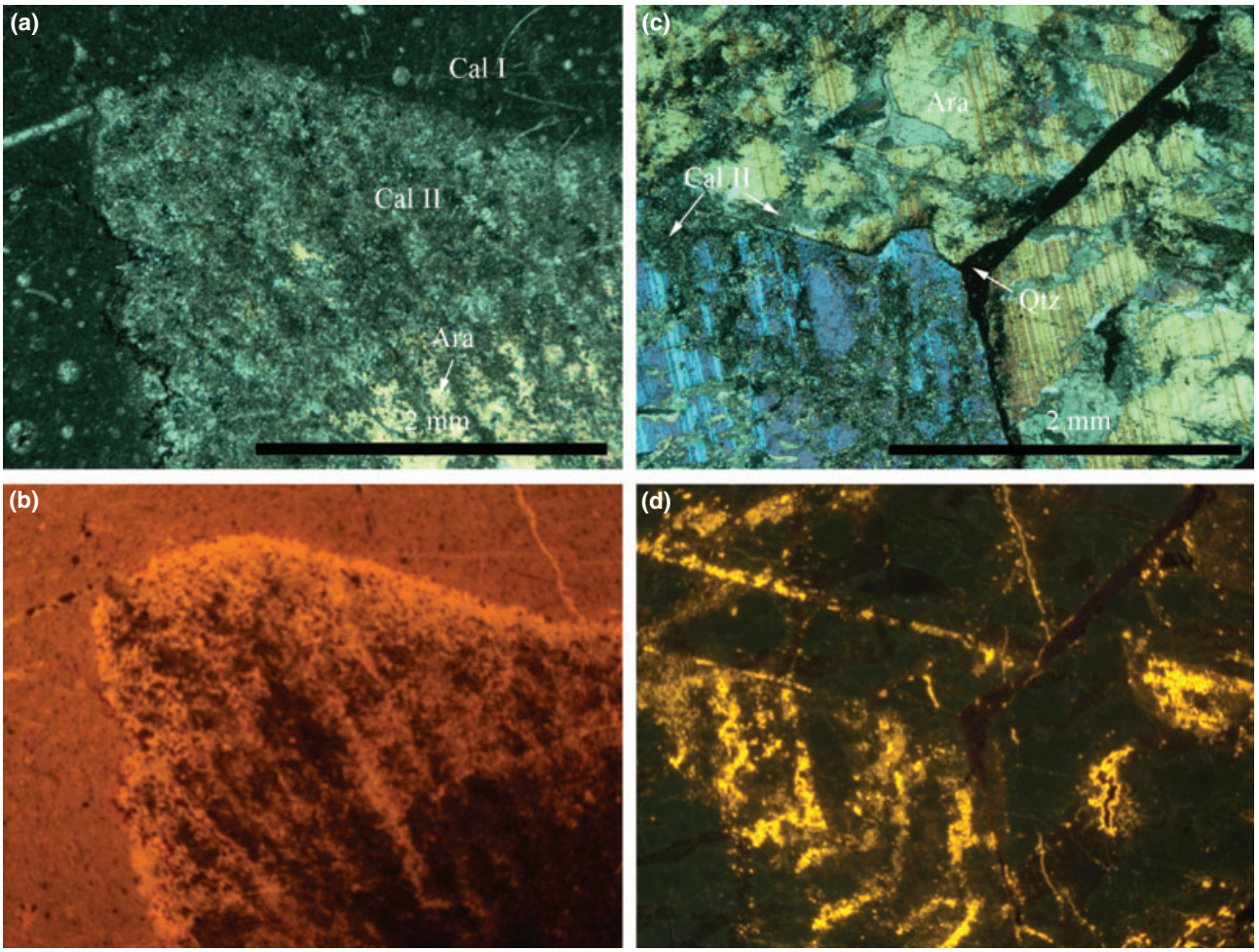

Fig. 6. (a) Optical micrograph of metamorphic aragonite (Ara) and relict micrite (Calcite I). Aragonite is partly transformed to calcite (Cal II). Crossed polarizers. (b) Cathodoluminescence picture of domain shown in panel a. (c) Aragonite crystals (partly transformed to Cal II) and intergranular quartz (Qtz). (d) Cathodoluminescence picture of domain shown in (c).

Table 2. Average composition of carbonates (mol.%; $\pm 1\sigma$) in aragonite-bearing high-*P*–*T* metamorphic limestones.

	Calcite I (micrite)				
	Upper/lower	Central	Aragonite	Calcite II (replacing Ara)	Calcite III (late veins)
$CaCO_3$	98.77 ± 0.41	98.88 ± 0.21	99.85 ± 0.14	99.88 ± 0.11	99.57 ± 0.16
$MgCO_3$	0.75 ± 0.25	0.73 ± 0.17	0.01 ± 0.02	0.01 ± 0.01	0.04 ± 0.03
$FeCO_3$	0.11 ± 0.12	0.10 ± 0.07	0.05 ± 0.08	0.04 ± 0.04	0.03 ± 0.03
$MnCO_3$	0.34 ± 0.25	0.27 ± 0.11	0.05 ± 0.06	0.04 ± 0.06	0.34 ± 0.15
$SrCO_3$	0.03 ± 0.04	0.03 ± 0.04	0.04 ± 0.06	0.03 ± 0.04	0.03 ± 0.05

curved grain boundaries (Figs 2d–f & 4a). Calcite III has relatively high contents of $MnCO_3$ (0.34 ± 0.15 mol.%; Table 2).

P–T CONDITIONS OF ARAGONITIZATION

Metamorphic *P*–*T* conditions can be estimated from the mineral assemblages (Na-pyroxene, pumpellyite, lawsonite, quartz, albite, chlorite and quartz) found in veins and amygdales of the basaltic pillows associated with aragonitized limestones. The reactions (1) stilbite = lawsonite + quartz + H_2O and (2) lawsonite + pumpellyite = zoisite + chlorite + quartz + H_2O suggest a temperature interval of ~ 140–250 °C (Liou *et al.*, 1985, 1987; Schiffman & Day, 1999). However, because of the Fe_2O_3-rich composition of the lawsonite (2.23–5.25 wt%) (Okay, 1982), these reactions should have occurred at lower temperatures in the Gümüşyeniköy area. At temperatures of 140–250 °C, the well-defined calcite to aragonite reaction indicates minimum pressures of 0.48–0.65 GPa (Johannes & Puhan, 1971; Hacker *et al.*, 2005). The jadeite component of the sodic pyroxene, associated with albite and quartz in the basaltic rocks, varies between 3 and 35 mol.%. The maximum jadeite component indicates a similar pressure of 0.50–0.65 GPa based on the reaction albite = jadeite + quartz (Holland, 1980, 1983). Thus, the best estimate for the

conditions of aragonitization is 140–250 °C and 0.45–0.65 GPa.

DISCUSSION

The main questions to be answered are why the aragonitization started selectively in the centre of the layers, and why aragonite nucleation was inhibited in the relict micritic domains. As described above, micritic calcite I has constant composition across the carbonate beds. This suggests that kinetic rather than thermodynamic factors were responsible for the selective aragonitization in the central portions of the beds. Incorporation of Mg, Fe and Mn stabilizes calcite to higher pressures, while the addition of Sr enlarges the stability field of aragonite to lower pressures (Carlson, 1980; Lin & Huang, 2004; Hacker *et al.*, 2005). The shift of the calcite to aragonite reaction curve for a calcite with 1 mol.% $(Mg,Fe,Mn)CO_3$ as opposed to pure calcite is only $\sim$ 8 °C for a given pressure. The narrow width of the divariant field where $(Mg,Fe,Mn)CO_3$-bearing calcite and pure aragonite can stably coexist makes it highly unlikely that the incipient blueschist-facies metamorphism just fell in this range. Therefore, thermodynamic effects probably had little role in the arrested aragonitization of micritic calcite I, and it is reasonable to assume that micritic Cal I was a metastable phase in the aragonite stability field.

Experimental studies of Lin & Huang (2004) indicate that the transformation rate of the calcite-aragonite reaction depends on a number of factors including grain size, physical properties of grain boundaries, presence of impurity minerals, composition of the original carbonate, presence of a fluid phase, tectonic stress and amount of pressure and/or temperature overstep. In the carbonate rocks from Gümüşyeniköy, both the vast difference in grain size between the two carbonate minerals (up to 1200 times) and the absence of any aragonite in the relict micritic domains suggest that nucleation was an important kinetic factor in the formation of aragonite. Nucleation generally originates at local heterogeneities, such as grain boundaries, cleavage and twinning planes, internal fracture surfaces and subgrain boundaries. In experimental studies of the calcite-aragonite transformation, aragonite preferentially nucleated on grain boundaries due to their higher free energy relative to that of intragranular defects (e.g. Carlson & Rosenfeld, 1981; Carlson, 1983; Gillet *et al.*, 1987; Hacker *et al.*, 1992, 2005; Hacker & Kirby, 1993; Lin & Huang, 2004). In the rocks from Gümüşyeniköy, the generally very fine grain size of micritic Cal I should have provided a comparable large number of nucleation sites across the whole carbonate layer. Therefore, the effect of grain size cannot account for the observed retardation of aragonite formation in the upper and lower portions of the beds.

The addition of quartz grains to the calcite aggregates apparently increases the calcite to aragonite transformation rate, as shown by experimental work (Lin & Huang, 2004). This is ascribed to (i) local strain which can be induced by squeezing between the rigid quartz grains, and (ii) supply of more nucleation sites. In Gümüşyeniköy, quartz grains (sizes $\leq$25 μm) are found in both micritic and aragonitized portions with the difference that quartz is evenly dispersed in the micritic portions, and is found either as inclusion in aragonite or as clustered aggregates, together with Fe-Mn-hydroxides and clay minerals, along the grain boundaries in the aragonitized portion. The identical grain size of quartz in both micritic and aragonitic sections of the limestones indicate that the expulsion and accumulation of quartz grains at the grain boundaries are a physical process. Hence, the presence of quartz impurities cannot explain selective initiation of aragonitization in the central part of the limestone beds.

The difference in composition between $(Mg,Fe,Mn)CO_3$-bearing micritic calcite I and newly formed endmember aragonite (Table 2) indicates that aragonitization was not a pure phase transformation, but involved a net-transfer reaction by which additional phases, such as Mn-Fe-hydroxide, were formed. Unfortunately, the very small grain size of the Fe-Mn-hydroxides did not allow for precise analysis of these phases, making it impossible to distinguish between pre- and syn-aragonitization hydroxides. The general absence of dolomite implies that Mg was transported away, presumably by a fluid phase. The oxidation of Fe and Mn also implies the access of oxidizing components of fluids. In the presence of a free aqueous phase, mineral transformations occur via processes of solution and deposition (Brown *et al.*, 1962; Carlson & Rosenfeld, 1981, and references therein). Fluid flow is expected to occur preferentially along the shaly interlayers and fractures. Thus, aragonite nucleation and growth should have started along these structural elements, which, however, is clearly not the case in the micritic limestones of Gümüşyeniköy. On the other hand, reduction of the interface mobility by a larger amount of impurities (Fe-Mn-hydroxides, clay minerals, quartz) in the stylolite-rich upper and lower portions of the carbonate layers (due to preferential solution of calcite) may have retarded the growth rates of aragonite nuclei.

The transformation of aragonite to calcite during decompression may proceed at a variety of rates depending on temperature, pressure and grain size. Maximum temperatures for preserving aragonite when the retrograde *P–T* path enters the calcite stability field at geological rates may therefore differ. Estimates range from $\sim$ 500 °C (Wang & Liou, 1993) via $<$235 °C (Liu & Yund, 1993), 150–200 °C (Carlson & Rosenfeld, 1981) to $<$100 °C (Huang, 2003). As peak metamorphic temperatures of the investigated aragonite-bearing rocks from Gümüşyeniköy were lower than $\sim$ 250 °C, the preservation of aragonite in these rocks is not surprising. The fine-grained calcite (Cal

II), grown at the expense of large aragonite crystals, suggest that slow growth rate of Cal II rather than nucleation was responsible for the preservation of aragonite. This forms a contrast to the calcite-aragonite transformation where reaction rate is controlled by nucleation.

CONCLUSIONS

In the Tavşanlı Zone in north-west Turkey, partial aragonitization of bedded micritic limestones within an accretionary wedge occurred at very low-grade metamorphic conditions, and was preceded by stylolite formation. Aragonitization started at the centre of carbonate beds and proceeded towards the stylolite-rich upper and lower portions of the beds. In marked contrast to the very fine grain size of the micrite consisting of $(Mg,Mn,Fe)CO_3$-bearing calcite, aragonite forms large grains, up to 3 cm across, and has near-endmember composition. Constant composition of relict micritic calcite ($\sim$ 98–99 mol.% $CaCO_3$) across individual carbonate beds indicates that selective aragonitization in the central portions of the beds was controlled by kinetic rather than thermodynamic factors. In particular, nucleation and growth of aragonite in the upper and lower portions of the beds may have been retarded by the reduction of interface mobility due to a larger amount of mineral impurities (clay minerals, Fe-Mn-hydroxides). The carbonate rocks from the Tavşanlı Zone represent the first occurrence of incomplete prograde aragonitization of limestones during high-pressure metamorphism.

ACKNOWLEDGEMENTS

This paper has greatly benefited from the constructive and helpful reviews of J. Brady and W.D. Carlson, as well as from fruitful discussions with T. Zack. Special thanks are due to M.A. Oral and Y. Ilgar for cutting rock slices, I. Fin and O. Wienand for preparing numerous high-quality polished thin sections and rock slices. We are indebted to I. Glass and F. Lapponi for experimental help. The friendly accommodation provided by the Gümüşyeniköy villagers during the field work is gratefully acknowledged. A.I. Okay thanks the Turkish Academy of Sciences (TUBA) for partial financial support.

REFERENCES

Balz, M., Therese, H. A., Li, J. *et al.* 2005. Crystallization of vaterite nanowires by the cooperative interaction of tailor-made nucleation surfaces and polyelectrolytes. *Advanced Functional Materials*, **15,** 683–688.

Behrens, G., Kuhn, L. T., Ubic, R. & Heuer, A. H., 1995. Raman-spectra of vateritic calcium-carbonate. *Spectroscopy Letters*, **28,** 983–995.

Brady, J. B., Markley, M. J., Schumacher, J. C., Cheney, J. T. & Bianciardi, G. A., 2004. Aragonite pseudomorphs in high-pressure marbles of Syros, Greece. *Journal of Structural Geology*, **26,** 3–9.

Brothers, R. N., 1970. Lawsonite-albite schists from northernmost New Caledonia. *Contributions to Mineralogy and Petrology*, **25,** 185–202.

Brown, W. H., Fyfe, W. S. & Turner, F. J., 1962. Aragonite in California glaucophane schists, and the kinetics of the aragonite-calcite transformation. *Journal of Petrology*, **3,** 566–582.

Carlson, W. D., 1980. The calcite-aragonite equilibrium: effects of Sr substitution and anion orientational disorder. *American Mineralogist*, **65,** 1252–1262.

Carlson, W. D., 1983. Aragonite-calcite nucleation kinetics: an application and extension of Avrami transformation theory. *Journal of Geology*, **91,** 57–71.

Carlson, W. D. & Rosenfeld, J. L., 1981. Optical determination of topotactic aragonite-calcite growth kinetics: metamorphic implications. *Journal of Geology*, **89,** 615–638.

Coleman, R. G. & Lee, D. E., 1962. Metamorphic aragonite in the glaucophane schists of Cazadero, California. *American Journal of Science*, **260,** 577–595.

Droop, G. T. R., Karakaya, M. Ç., Eren, Y. & Karakaya, N., 2005. Metamorphic evolution of blueschists of the Altınekin complex, Konya area, south central Turkey. *Geological Journal*, **40,** 127–153.

Franz, L. & Okrusch, M., 1992. Aragonite-bearing blueschists on Arkai island, Dodecanese, Greece. *European Journal of Mineralogy*, **4,** 527–537.

Gillet, P. & Goffé, B., 1988. On the significance of aragonite occurrences in the Western Alps. *Contributions to Mineralogy and Petrology*, **99,** 70–81.

Gillet, P., Gerard, Y. & Willaime, C., 1987, The calcite-aragonite transition: mechanism and microstructures induced by the transformation stresses and strain. *Bulletin Minéralogique*, **110,** 481–496.

Hacker, B. R. & Kirby, S. H., 1993. High-pressure deformation of calcite-marble and its transformation to aragonite under non-hydrostatic conditions. *Journal of Structural Geology*, **15,** 1207–1222.

Hacker, B. R., Kirby, S. H. & Bohlen, S. R., 1992. Time and metamorphic petrology: calcite to aragonite experiments. *Science*, **258,** 110–112.

Hacker, B. R., Abers, G. A. & Peacock, S. M., 2003. Subduction factory I. Theoretical mineralogy, densities, seismic wave speeds and H_2O contents. *Journal of Geophysical Research*, **108,** B12029, DOI 10.1029/2001JB001127.

Hacker, B. R., Rubie, D. C., Kirby, S. H. & Bohlen, S. R., 2005. The calcite $\rightarrow$ aragonite transformation in low-Mg marble: equilibrium relations, transformation mechanism, and the rates. *Journal of Geophysical Research*, **110,** B03205, DOI 10.1029/20004JB003302.

Holland, T. J. B., 1980. The reaction albite = jadeite + quartz determined experimentally in the range 600–1200 °C. *American Mineralogist*, **65,** 129–134.

Holland, T. J. B., 1983. Experimental determination of activities in disordered and short-range ordered jadeitic pyroxenes. *Contributions to Mineralogy and Petrology*, **82,** 214–220.

Huang, W.-L., 2003. Synthetic polycrystalline aragonite to calcite transformation kinetics: experiments at pressures close to the equilibrium boundary. *Mineralogy and Petrology*, **79,** 243–258.

Johannes, W. & Puhan, D., 1971. The calcite-aragonite transition, reinvestigated. *Contributions to Mineralogy and Petrology*, **31,** 28–38.

Kerrick, D. M. & Connolly, J. A. D., 2001. Metamorphic devolatilization of subducted oceanic metabasalts: implications for seismicity, arc magmatism and volatile recycling. *Earth and Planetary Science Letters*, **189,** 19–29.

Lin, S.-J. & Huang, W.-L., 2004. Polycrystalline calcite to aragonite transformation kinetics: experiments in synthetic systems. *Contributions to Mineralogy and Petrology*, **147,** 604–614.

Liou, J. G., Maruyama, S. & Cho, M., 1985. Phase equilibria and mineral parageneses of metabasites in low-grade metamorphism. *Mineralogical Magazine*, **49,** 321–333.

Liou, J. G., Maruyama, S. & Cho, M., 1987. Very low-grade metamorphism of volcanic and volcaniclastic rocks – mineral assemblages and mineral facies. In: *Low Temperature Metamorphism* (ed. Frey, M.), pp. 59–113, Blackie & Son, Glasgow.

Liu, M. & Yund, R. A., 1993. Transformation kinetics of polycrystalline aragonite to calcite: new experimental data, modeling and implications. *Contributions to Mineralogy and Petrology*, **114,** 465–478.

Martinez-Ramirez, S., Sanchez-Cortes, S., Garcia-Ramos, J. V., Domingo, C., Fortes, C. & Blanco-Varela, M. T., 2003. Micro-Raman spectroscopy applied to depth profiles of carbonates formed in lime mortar. *Cement and Concrete Research*, **33,** 2063–2068.

McKee, B., 1962. Aragonite in the Franciscan rocks of the Pacheco Pass area, California. *American Mineralogist*, **47,** 379–387.

Nasdala, L., Hanchar, J.-M., Kronz, A. & Whitehouse, M. J., 2005. Long-term stability of alpha particle damage in natural zircon. *Chemical Geology*, **220,** 83–103.

Newton, R. C., Goldsmith, J. R. & Smith, J. V., 1969. Aragonite crystallization from strained calcite at reduced pressures and its bearing on aragonite in low-grade metamorphism. *Contributions to Mineralogy and Petrology*, **22,** 335–348.

Okay, A. I., 1982. Incipient blueschist metamorphism and metasomatism in the Tavşanlı region, northwest Turkey. *Contributions to Mineralogy and Petrology*, **79,** 361–367.

Okay, A. I., 1986. High pressure/low temperature metamorphic rocks of Turkey. In: *Blueschists and Eclogites* (eds Evans, B.W. & Brown, E.H.), *Geological Society of America Memoir*, **164,** 333–348.

Okay, A. I., 2002. Jadeite-choritoid-glaucophane-lawsonite blueschists in north-east Turkey: unusually high P/T ratios in continental crust. *Journal of Metamorphic Geology*, **20,** 757–768.

Poli, S. & Schmidt, M. W., 2002. Petrology of subducted slabs. *Annual Review of Earth and Planetary Sciences*, **30,** 207–235.

Pouchou, J. L. & Pichoir, F., 1984. A new model for quantitative analyses. I. Application to the analysis of homogeneous samples. *La Recherche Aérospatiale*, **3,** 13–38.

Pouchou, J. L. & Pichoir, F., 1985. 'PAP' (ϕ-ρ-Z) correction procedure for improved quantitative microanalysis. In: *Microbeam Analysis* (ed. Armstrong, J.T.), pp. 104–106, San Francisco Press, San Francisco, CA.

Rubie, D. C., 1998. Disequilibrium during metamorphism: the role of the nucleation kinetics. In: *What Drives Metamorphism and Metamorphic Reactions?* (eds Treloar, P.J. & O'Brien, P.), *Geological Society, London, Special Publications*, **138,** 199–214.

Sakakibara, M., 1986. A newly discovered high-pressure terrane in the Eastern Hokkaido, Japan. *Journal of Metamorphic Geology*, **4,** 401–408.

Schiffman, P. & Day, H. W., 1999. Petrological methods for the study of very low-grade metabasites. In: *Low-Grade Metamorphism* (eds Frey, M. & Robinson, D.), pp. 108–142. Blackwell Science, Oxford.

Sherlock, S., Kelley, S., Inger, S., Harris, N. & Okay, A. I., 1999. ^{40}Ar-^{39}Ar and Rb-Sr geochronology of high-pressure metamorphism and exhumation history of the Tavşanlı Zone. *Contributions to Mineralogy and Petrology*, **137,** 46–58.

Theye, T. & Seidel, E., 1993. Uplift-related retrogression history of aragonite marbles in Western Crete (Greece). *Contributions to Mineralogy and Petrology*, **114,** 349–356.

Urmos, J., Sharma, S. K. & Mackenzie, F. T., 1991. Characterization of some biogenic carbonates with Raman spectroscopy. *American Mineralogist*, **76,** 641–646.

Wang, X. & Liou, J. G., 1993. Ultrahigh pressure metamorphism of carbonate from Dabie Mountains, Central China. *Journal of Metamorphic Geology*, **11,** 575–588.

Received 17 February 2006; revision accepted 13 June 2006.